

Coorbital thermal torques on low-mass protoplanets

Frédéric S. Masset[★]

Instituto de Ciencias Físicas, Universidad Nacional Autónoma de México, Av. Universidad s/n, 62210 Cuernavaca, Mor., Mexico

Accepted XXX. Received YYY; in original form ZZZ

ABSTRACT

Using linear perturbation theory, we investigate the torque exerted on a low-mass planet embedded in a gaseous protoplanetary disc with finite thermal diffusivity. When the planet does not release energy into the ambient disc, the main effect of thermal diffusion is the softening of the enthalpy peak near the planet, which results in the appearance of two cold and dense lobes on either side of the orbit, of size smaller than the thickness of the disc. The lobes exert torques of opposite sign on the planet, each comparable in magnitude to the one-sided Lindblad torque. When the planet is offset from corotation, the lobes are asymmetric and the planet experiences a net torque, the ‘cold’ thermal torque, which has a magnitude that depends on the relative value of the distance to corotation to the size of the lobes $\sim \sqrt{\chi/\Omega_p}$, χ being the thermal diffusivity and Ω_p the orbital frequency. We believe that this effect corresponds to the phenomenon named ‘cold finger’ recently reported in numerical simulations, and we argue that it constitutes the dominant mode of migration of sub-Earth-mass objects. When the planet is luminous, the heat released into the ambient disc results in an additional disturbance that takes the form of hot, low-density lobes. They give a torque, named heating torque in previous work, that has an expression similar, but of opposite sign, to the cold thermal torque.

Key words: planet-disc interactions – protoplanetary discs – hydrodynamics – diffusion – planets and satellites: formation.

1 INTRODUCTION

The dependence on thermal diffusion of the torque experienced by a planet embedded in a gaseous disc has been investigated mainly for planet masses ranging from a few tens of Earth masses down to a few Earth masses. In this mass range, a complex dependence of the torque on thermal diffusivity has been found, which has been accounted for by the non-linear dynamics of the corotation torque (Masset & Casoli 2010; Paardekooper et al. 2011). Such studies have been tackled by means of a mixture of numerical simulations and toy models of the coorbital region. The more direct impact of thermal diffusivity on the linearized equations of the flow, however, has never been investigated. Most analytic studies of the angular momentum exchange between an external perturber and the gaseous disc have either assumed the gas to be isothermal, or, when relaxing this barotropic assumption, to behave adiabatically. In recent numerical simulations, Lega et al. (2014) argue for the existence of a hitherto unmentioned component of the torque between a low-mass planet and a gaseous disc, which they attribute to the existence of thermal diffusion. This torque is found to originate

from regions located in the immediate vicinity of the planet, well within the length-scale of pressure. In these regions, the gas is colder and more dense than it would be if it behaved adiabatically. These regions are found on both sides of corotation, and exert torques of opposite signs. Because of an asymmetry between the torque of the inner and outer regions, they exert a net torque. The authors dubbed this effect the ‘cold finger’ effect. In a different spirit, Benítez-Llambay et al. (2015) have studied the impact on migration of heat release by low-mass, luminous planets. Thermal diffusion is naturally an essential ingredient of such study. They find that the heat released in the vicinity of the planet diffuses in the nearby disc and is carried away by the Keplerian flow, yielding in steady state two hot, low-density lobes. These lobes share a number of properties with the regions identified by Lega et al. (2014): their characteristic size is smaller than the length-scale of pressure, they exert antagonistic torques on the planet, and they are asymmetric, so that they exert a net torque on the planet. Since the regions identified by Lega et al. (2014) and those found by Benítez-Llambay et al. (2015) have similar properties but correspond to perturbations of opposite signs (the former are dense and cold, the latter are hot and underdense), it is not surprising that the net torques found in these two works have opposite signs: while Lega et al. (2014) find their additional torque

[★] masset@icf.unam.mx

component to be negative, [Benítez-Llambay et al. \(2015\)](#) find that the release of heat increases the total torque on the planet, up to the point that it can become positive if the luminosity is sufficiently large. Motivated by these findings, we undertake here the study of the torque experienced by a low-mass planet in a disc with a finite thermal diffusivity, using linear perturbation theory in a three-dimensional (3D) shearing sheet (we anticipate curvature effects to be unimportant, owing to the small size of the disturbances and their proximity to the planet). We lay down our assumptions and write our governing equations in section 2. We then first turn to a study of the heat release in section 3. While it may seem at first glance that dealing with the additional complexity of heat release should be studied after the response to a cold planet, it is actually simpler, and provides hints to the solution for a massive, non-luminous object, which we consider in section 4. In that section we evaluate the impact of a finite thermal diffusivity on the torque experienced by a low-mass, non-luminous planet. In section 5, we discuss our results and compare the magnitude of the effect we found to that of the Lindblad and corotation torques on a low-mass planet. We draw our conclusions in section 6.

2 BASIC EQUATIONS

2.1 Main assumptions

We consider a planet of mass M embedded in a protoplanetary disc on a circular, prograde and non-inclined orbit of radius r_p . The central star has a mass M_\star , the disc has a surface density Σ and an angular velocity $\Omega(r)$, where r is the distance to the central star. We assume that the disturbances that are the subject of the present study are small compared to the pressure length-scale H of the disc. We will assess in section 5 the extent to which this assumption is justified. This assumption allows us to perform our study in the framework of the shearing sheet ([Narayan et al. 1987](#)), here in three dimensions¹. Our frame is essentially a Cartesian box of dimensions much smaller than the planet's orbital radius, which contains the planet and corotates with it. We use the conventional notation for the axes: x is directed along the gradient of unperturbed velocity (i.e. along the radial direction from a global perspective), y is directed along the unperturbed motion (i.e. along the azimuthal direction) and z is perpendicular to the disc's midplane. Although the direction of the central object is unspecified in the shearing sheet, we will refer to the material at $x > 0$ ($x < 0$) as the outer (inner) disc, implying that the central object lies on the negative side of the x -axis. The planet location is $(x, y, z) = (x_p, 0, 0)$. The vanishing value of z arises from the assumption of an orbit coplanar with the disc, while y can be set to 0 without loss of generality.

The continuity equation reads:

$$\partial_t \rho + \nabla \cdot (\rho \mathbf{V}) = 0, \quad (1)$$

¹ In the literature, the expression ‘‘shearing box’’, which would be more appropriate, almost always refer to a numerical device, used in particular in local magnetohydrodynamics simulations, rather than to the framework proposed by [Narayan et al.](#)

where ρ is the density and $\mathbf{V} = (u, v, w)^T$ the velocity. The Euler equation reads

$$\partial_t \mathbf{V} + \mathbf{V} \cdot \nabla \mathbf{V} + 2\Omega_p \mathbf{e}_z \times \mathbf{V} = -\nabla(\Phi_t + \Phi_p) - \frac{\nabla p}{\rho}, \quad (2)$$

where \mathbf{e}_z is the unit vector along the z -axis, Ω_p is the rotation rate of the frame about this axis, Φ_p is the planetary potential and p is the pressure. In Eq. (2), $\Phi_t = -q\Omega_p^2(x - x_p)^2 + (1/2)\Omega_p^2 z^2$ is the tidal potential, q being a dimensionless number that quantifies the shear ($q = 3/2$ in Keplerian discs). Finally, the equation for the density of internal energy e reads:

$$\partial_t e + \nabla \cdot (e \mathbf{V}) = -p \nabla \cdot \mathbf{V} - \nabla \cdot \mathbf{F}_H + S, \quad (3)$$

where $S = S_0(\mathbf{r}) + S_p(\mathbf{r})$ is a source term that consists of the source terms S_0 of the unperturbed disc and S_p arising from the release of energy into the gas by the planet, and where \mathbf{F}_H is the heat flux, given by

$$\mathbf{F}_H = -\chi \rho \nabla \left(\frac{e}{\rho} \right), \quad (4)$$

where χ is the thermal diffusivity. We assume the gas to be ideal and write

$$p = (\gamma - 1)e, \quad (5)$$

where γ is the adiabatic index. We write the perturbed quantities as the sum of the unperturbed value and a perturbation, denoted with a prime:

$$\rho = \rho_0 + \rho' \quad (6)$$

$$e = e_0 + e' \quad (7)$$

$$p = p_0 + p' \quad (8)$$

$$u = u' \quad (9)$$

$$v = v_0 + v' = -q\Omega_p x + v' \quad (10)$$

$$w = w', \quad (11)$$

where Eq. (10) arises from Eq. (2) with the choice that $v_0 = 0$ for $x = 0$ (the plane $x = 0$ is therefore the planet's corotation), which implies

$$x_p = -\frac{\partial_x p_0}{2q\Omega_p^2 \rho_0}. \quad (12)$$

From now on we make the assumption that x_p , which is the distance of the planet to its corotation, is much smaller than the size of the disturbance. We linearize Eqs. (1)-(3) and assume a steady state. We obtain

$$-q\Omega_p x \partial_y \rho' + \rho_0 (\partial_x u' + \partial_y v' + \partial_z w') = 0 \quad (13)$$

$$-q\Omega_p x \partial_y u' - 2\Omega_p v' = -\frac{\partial_x p'}{\rho_0} + \frac{(\partial_x p_0) \rho'}{\rho_0^2} - \partial_x \Phi_p \quad (14)$$

$$-q\Omega_p x \partial_y v' + (2 - q)\Omega_p u' = -\frac{\partial_y p'}{\rho_0} - \partial_y \Phi_p \quad (15)$$

$$-q\Omega_p x \partial_y w' = -\frac{\partial_z p'}{\rho_0} + \frac{(\partial_z p_0) \rho'}{\rho_0^2} - \partial_z \Phi_p \quad (16)$$

$$\begin{aligned} -q\Omega_p x \partial_y p' + \gamma p_0 (\partial_x u' + \partial_y v' + \partial_z w') \\ = \chi \Delta p' - \chi \frac{p_0}{\rho_0} \Delta \rho' + (\gamma - 1) S_p(\mathbf{r}), \end{aligned} \quad (17)$$

where we have used Eq. (5) to eliminate all instances of e , and where we have assumed the size of the perturbation to be much smaller than the length-scale over which the unperturbed quantities vary. The second term of the right-hand side of Eq. (16) is therefore typically smaller by a factor of order $(\lambda/H)^2$ than the preceding term, and we neglect it. This amounts to neglecting the vertical stratification of the disc. We take the Fourier transform of the perturbations in y and z , with the following conventions of sign and normalization:

$$\tilde{\xi}(x, k_y, k_z) = \iint \xi'(x, y, z) e^{-i(k_y y + k_z z)} dy dz \quad (18)$$

$$\xi'(x, y, z) = \frac{1}{4\pi^2} \iint \tilde{\xi}(x, k_y, k_z) e^{i(k_y y + k_z z)} dk_y dk_z, \quad (19)$$

where ξ' represents the perturbation of an arbitrary variable, and $\tilde{\xi}$ its two-dimensional Fourier transform. The system of Eqs. (13)-(17) can therefore be rewritten as the following system of ordinary differential equations:

$$-iqk_y \Omega_p x \tilde{\rho} + \rho_0 (\partial_x \tilde{u} + ik_y \tilde{v} + ik_z \tilde{w}) = 0 \quad (20)$$

$$-iqk_y \Omega_p x \tilde{u} - 2\Omega_p \tilde{v} + \frac{\partial_x \tilde{p}}{\rho_0} - \frac{\partial_x p_0}{\rho_0^2} \tilde{\rho} = -\partial_x \tilde{\Phi}_p \quad (21)$$

$$-iqk_y \Omega_p x \tilde{v} + (2-q)\Omega_p \tilde{u} + \frac{ik_y \tilde{p}}{\rho_0} = -ik_y \tilde{\Phi}_p \quad (22)$$

$$-iqk_y \Omega_p x \tilde{w} + \frac{ik_z \tilde{p}}{\rho_0} = -ik_z \tilde{\Phi}_p \quad (23)$$

$$\begin{aligned} -iqk_y \Omega_p x \tilde{p} + \gamma p_0 (\partial_x \tilde{u} + ik_y \tilde{v} + ik_z \tilde{w}) \\ - \chi \Delta' \tilde{p} + \frac{\chi c_s^2}{\gamma} \Delta' \tilde{\rho} = (\gamma - 1) \tilde{S}_p, \end{aligned} \quad (24)$$

where we have written the forcing terms arising from the planet on the right-hand side and where c_s is the adiabatic sound speed:

$$c_s = \sqrt{\frac{\gamma p_0}{\rho_0}}. \quad (25)$$

In Eq. (24), the Δ' operator is

$$\Delta' \equiv \frac{\partial^2}{\partial x^2} - k^2, \quad (26)$$

with

$$k^2 = k_y^2 + k_z^2 \quad (27)$$

Finally, we can use Eq. (20) to eliminate the divergence of velocity in Eq. (24) and obtain

$$-iqk_y \Omega_p x (\tilde{p} - c_s^2 \tilde{\rho}) - \chi \Delta' \left(\tilde{p} - \frac{c_s^2}{\gamma} \tilde{\rho} \right) = (\gamma - 1) \tilde{S}_p. \quad (28)$$

This relationship constitutes our main equation in what follows.

In the following section, we further simplify this relation by showing that for disturbances (i) that are not triggered by a potential and (ii) that are much smaller than the length-scale of pressure, the relative perturbation of pressure is negligible compared to that of density, so that Eq. (28) can take a particularly simple form.

2.2 Magnitude of the perturbation of pressure

Using Eqs. (21)-(23), we can obtain the expression of \tilde{u} , \tilde{v} and \tilde{w} as a function of \tilde{p} , $\tilde{\Phi}_p$ and their derivatives in x . These can be substituted in Eq. (20), so as to yield an expression of $\tilde{\rho}$ as a function of \tilde{p} and $\tilde{\Phi}_p$. We obtain

$$\tilde{\rho} - \frac{1}{D\Omega_p^2} \frac{\partial_x p_0}{\rho_0} \partial_x \tilde{\rho} = \mathcal{L} \left(\tilde{\Phi}_p + \frac{\tilde{p}}{\rho_0} \right) \quad (29)$$

where the dimensionless quantity D is

$$D = q^2 k_y^2 x^2 - 2(2-q). \quad (30)$$

and where the linear operator \mathcal{L} is defined by

$$\begin{aligned} \mathcal{L}(Y) = - \frac{\rho_0}{D\Omega_p^2} \partial_{x^2}^2 Y + \frac{2\rho_0 q^2 k_y^2 x}{D^2 \Omega_p^2} \partial_x Y \\ + \rho_0 \left[\frac{k_y^2}{D\Omega_p^2} \left(1 - \frac{4q}{D} \right) + \frac{k_z^2}{q^2 k_y^2 \Omega_p^2 x^2} \right] Y. \end{aligned} \quad (31)$$

Using Eq. (12), Eq. (29) can be recast as

$$\tilde{\rho} + \frac{qx_p}{2D} \partial_x \tilde{\rho} = \mathcal{L} \left(\tilde{\Phi}_p + \frac{\tilde{p}}{\rho_0} \right). \quad (32)$$

Under our assumption that x_p is much smaller than the typical size of the disturbance, the second term of the left-hand side is negligible compared to the first one since q and D are of order unity, and we can write

$$\tilde{\rho} \approx \mathcal{L} \left(\tilde{\Phi}_p + \frac{\tilde{p}}{\rho_0} \right). \quad (33)$$

We now specify to the case of a perturbation not triggered by a gravitational potential, which therefore obeys:

$$\tilde{\rho} \approx \mathcal{L} \left(\frac{\tilde{p}}{\rho_0} \right). \quad (34)$$

An order of magnitude of the perturbation of pressure can be obtained by letting $k_y^{-1} \sim k_z^{-1} \sim x \sim \lambda$, $\partial_x \tilde{p} \sim p/H$ and $\partial_{x^2}^2 \tilde{p} \sim \tilde{p}/H^2$, $\lambda \ll H$ being the typical size of the density disturbance. The third and last term of the right-hand side of Eq. (31) is then dominant and implies

$$\tilde{p} = O(\lambda^2 \Omega_p^2 \tilde{\rho}). \quad (35)$$

As a consequence, we have

$$\tilde{p} \ll H^2 \Omega_p^2 \tilde{\rho} \sim c_s^2 \tilde{\rho}. \quad (36)$$

This relation is valid for any disturbance smaller than the pressure length-scale that verifies Eq. (34).

2.3 Forcing terms

Having assumed that the distance of the planet to corotation $|x_p|$ is small compared to the size of the disturbance, we perform an expansion to first order in x_p of the planetary potential and heating term.

The former can be obtained taking the inverse Fourier transform in x of its three-dimensional Fourier transform $\tilde{\Phi}_p(x_p, k_x, k_y, k_z)$, which is readily obtained from Poisson's equation:

$$\tilde{\Phi}_p(x_p, k_x, k_y, k_z) = - \frac{4\pi G M e^{-ik_x x_p}}{k_x^2 + k_y^2 + k_z^2}, \quad (37)$$

which gives

$$\begin{aligned}\tilde{\Phi}(x_p, x, k_y, k_z) &= \frac{1}{2\pi} \int_{-\infty}^{+\infty} \tilde{\Phi}_p(x_p, k_x, k_y, k_z) e^{ik_x x} dk_x \\ &= -\frac{2\pi GM}{k} e^{-k|x-x_p|}.\end{aligned}\quad (38)$$

In the expansion of this expression, some care must be taken that the function $\exp(k|x-x_p|)$ does not have the same value for its left and right derivatives at $x_p = x$. We get

$$\tilde{\Phi}(x_p, x, k_y, k_z) = \Phi_p^{(0)}(x, k_y, k_z) + x_p \Phi_p^{(1)}(x, k_y, k_z) + O(x_p^2) \quad (39)$$

with

$$\Phi_p^{(0)}(x, k_y, k_z) = -\frac{2\pi GM}{k} e^{-k|x|} \quad (40)$$

and

$$\Phi_p^{(1)}(x, k_y, k_z) = -2\pi GM \operatorname{sgn}(x) e^{-k|x|}. \quad (41)$$

Similarly, specializing to a singular heat release at the planet's location:

$$S_p(x_p, r) = L\delta(x-x_p)\delta(y)\delta(z), \quad (42)$$

where δ is Dirac's distribution and L is the luminosity of the planet, we obtain:

$$\tilde{S}_p(x_p, x, k_y, k_z) = \tilde{S}_p^{(0)}(x, k_y, k_z) + x_p \tilde{S}_p^{(1)}(x, k_y, k_z) + O(x_p^2) \quad (43)$$

with

$$\tilde{S}_p^{(0)}(x, k_y, k_z) \equiv \tilde{S}_p^{(0)}(x) = L\delta(x) \quad (44)$$

and

$$\tilde{S}_p^{(1)}(x, k_y, k_z) \equiv \tilde{S}_p^{(1)}(x) = -L\delta'(x), \quad (45)$$

where we have reduced the set of independent variables of these two functions, as de facto they only depend on x .

2.4 Decomposition of the response of the disc

We can formally write the linear system of Eqs. (20) to (24) under the concise form:

$$S(\mathbf{Q}) = \mathbf{T}_\Phi + \mathbf{T}_H, \quad (46)$$

where

$$\mathbf{Q} = (\rho, u, v, w, e)^T, \quad (47)$$

$$\mathbf{T}_\Phi = (0, -\partial_x \tilde{\Phi}_p, -ik_y \tilde{\Phi}_p, -ik_z \tilde{\Phi}_p, 0)^T, \quad (48)$$

$$\mathbf{T}_H = (0, 0, 0, 0, \tilde{S}_p)^T \quad (49)$$

are respectively the vector of the solution, and the forcing terms arising from the planet's gravity and luminosity. In Eq. (46), S represents the linear operator corresponding the left-hand side of the set of Eqs. (20) to (24). Owing to the linearity of S , we can decompose the solution \mathbf{Q} as

$$\mathbf{Q} = \mathbf{Q}_\Phi + \mathbf{Q}_H, \quad (50)$$

where \mathbf{Q}_Φ and \mathbf{Q}_H verify respectively

$$S(\mathbf{Q}_\Phi) = \mathbf{T}_\Phi \quad (51)$$

and

$$S(\mathbf{Q}_H) = \mathbf{T}_H \quad (52)$$

When they fulfil appropriate boundary conditions, \mathbf{Q}_Φ and \mathbf{Q}_H characterize the disturbances excited respectively by

the planet's gravity and by the release of energy in the surrounding gas.

We can use the expansions of section 2.3 to further decompose the response of the disc. Using Eqs. (43) and (49), we can write

$$\mathbf{T}_H = \mathbf{T}_H^{(0)} + x_p \mathbf{T}_H^{(1)} + O(x_p^2), \quad (53)$$

with

$$\mathbf{T}_H^{(0)} = [0, 0, 0, 0, L\delta(r)]^T \quad (54)$$

$$\mathbf{T}_H^{(1)} = [0, 0, 0, 0, -L\delta'(r)]^T. \quad (55)$$

The linearity of the operator S implies that if we define $\mathbf{Q}_H^{(0)}$ and $\mathbf{Q}_H^{(1)}$ as solutions of the linear system respectively, with forcing terms $\mathbf{T}_H^{(0)}$ and $\mathbf{T}_H^{(1)}$,

$$S[\mathbf{Q}_H^{(0)}] = \mathbf{T}_H^{(0)} \quad (56)$$

$$S[\mathbf{Q}_H^{(1)}] = \mathbf{T}_H^{(1)}, \quad (57)$$

then $\mathbf{Q}_H^{(0)} + x_p \mathbf{Q}_H^{(1)}$ is an expansion to first order in x_p of the solution \mathbf{Q}_H of Eq. (52). A similar decomposition can be applied to the solution of Eq. (51), but it will not be required in the following.

3 EFFECT OF HEAT RELEASE

We first study the case of a luminous planet and work out the first-order expansion $\mathbf{Q}_H^{(0)} + x_p \mathbf{Q}_H^{(1)}$ of the solution \mathbf{Q}_H to the equation (52). It corresponds to a disturbance that yields a force which, by construction, is the difference of the force exerted on a luminous planet and the force exerted on a non-luminous planet. This corresponds to the torque component dubbed heating torque by Benítez-Llambay et al. (2015). In this whole section, we do not write an H index for the different hydrodynamic variables in order to improve legibility, but it must be understood that they are components of \mathbf{Q}_H .

3.1 Advection-diffusion equation

Since in this whole section we consider only the release of heat, the perturbations of density and pressure verify Eq. (34), and Eq. (36) holds. We can therefore neglect the two occurrences of \tilde{p} in Eq. (28), which takes the simple form

$$ik_y \Omega_p x \tilde{\rho} + \frac{\chi}{\gamma} \Delta' \tilde{\rho} = \frac{\gamma-1}{c_s^2} \tilde{S}_p, \quad (58)$$

This relation is equivalent, in real space, to

$$\mathbf{V}_0 \cdot \nabla \rho' = \frac{\chi}{\gamma} \Delta \rho' - \frac{\gamma-1}{c_s^2} S_p \quad (59)$$

Under the assumption $\lambda \ll H$ to which we have restricted ourselves, the perturbation of density is therefore solution of the simple diffusion-advection equation above, in which the advective velocity is the unperturbed velocity of the shearing sheet, while the pressure is essentially unperturbed ($|\rho'/\rho_0| \ll |\rho'/\rho_0|$).

We can decompose the Fourier transform of the density perturbation into its real and imaginary parts:

$$\tilde{\rho}(x, k_y, k_z) = \tilde{\rho}_R(x, k_y, k_z) + i\tilde{\rho}_I(x, k_y, k_z), \quad (60)$$

where $\tilde{\rho}_R$ and $\tilde{\rho}_I$ are real numbers. Eq. (58) is equivalent to the differential system:

$$-q\Omega_p k_y \gamma x \tilde{\rho}_I = -\chi[\partial_x^2 \tilde{\rho}_R - k^2 \tilde{\rho}_R] + \frac{\gamma(\gamma-1)\tilde{\delta}_p}{c_s^2} \quad (61)$$

$$q\Omega_p k_y \gamma x \tilde{\rho}_R = -\chi[\partial_x^2 \tilde{\rho}_I - k^2 \tilde{\rho}_I]. \quad (62)$$

We define the dimensionless quantity K as

$$K = \frac{\chi k^3}{q\Omega_p k_y \gamma}, \quad (63)$$

and introduce the new variable X as

$$X = xk, \quad (64)$$

which allows us to recast the system of Eqs. (61) and (62) as

$$X\tilde{\rho}_I = K(\tilde{\rho}_R'' - \tilde{\rho}_R) - \frac{(\gamma-1)k\tilde{\delta}_p}{q\Omega_p k_y c_s^2} \quad (65)$$

$$-X\tilde{\rho}_R = K(\tilde{\rho}_I'' - \tilde{\rho}_I), \quad (66)$$

where the symbol '' denotes the second derivative with respect to X . The boundary conditions that the solution must satisfy are

$$\tilde{\rho}_R \rightarrow 0 \quad \text{when } X \rightarrow \pm\infty \quad (67)$$

$$\tilde{\rho}_I \rightarrow 0 \quad \text{when } X \rightarrow \pm\infty \quad (68)$$

The real part $\tilde{\rho}_R$ has same parity in X as $\tilde{\delta}$, whereas the imaginary part $\tilde{\rho}_I$ has the opposite parity. Equations (65) and (66) describe the general response of the gas to an arbitrary heat function $\tilde{\delta}$, when the size of the disturbance is much smaller than the pressure length-scale.

3.2 Force expression

The force exerted on the planet by the perturbed density of a slab ranging from x_{\min} to x_{\max} has the expression

$$F_y = \int_{x_{\min}}^{x_{\max}} \int_{-\infty}^{\infty} \int_{-\infty}^{\infty} \rho' \partial_y \Phi_p dy dz dx \quad (69)$$

which can be recast, using Parseval's theorem, as

$$F_y = \frac{1}{\pi^2} \int_{x_{\min}}^{x_{\max}} dx \int_{k_y > 0} dk_y \int_{k_z > 0} dk_z \tilde{\Phi}_p k_y \tilde{\rho}_I, \quad (70)$$

where $\tilde{\rho}_I$, as in the previous section, represents the imaginary part of $\tilde{\rho}$, and where the front coefficient comes from our conventions of Eqs. (18) and (19). We have used the fact that ρ is even in z , and the fact that $\tilde{\Phi}_p$ is real and even in k_y and k_z to write the integral of Eq. (70) over the quadrant $k_y > 0, k_z > 0$.

Denoting with $\tilde{\rho}^{(0)}$ and $\tilde{\rho}^{(1)}$ respectively the density component of $\mathbf{Q}_H^{(0)}$ and $\mathbf{Q}_H^{(1)}$ defined at Eqs. (56) and (57), we can write, using the expansion of the potential of Eq. (39), the expansion of the force as

$$F_y = F_y^{(0)} + x_p F_y^{(1)} + O(x_p^2), \quad (71)$$

where

$$F_y^{(0)} = \frac{1}{\pi^2} \int_{x_{\min}}^{x_{\max}} dx \iint_{k_y > 0, k_z > 0} dk_y dk_z \tilde{\Phi}_p^{(0)} k_y \tilde{\rho}_I^{(0)} \quad (72)$$

and

$$F_y^{(1)} = \frac{1}{\pi^2} \int_{x_{\min}}^{x_{\max}} dx \iint_{k_y > 0, k_z > 0} dk_y dk_z k_y [\tilde{\Phi}_p^{(0)} \tilde{\rho}_I^{(1)} + \tilde{\Phi}_p^{(1)} \tilde{\rho}_I^{(0)}]. \quad (73)$$

When the limits of integration are $(x_{\min}, x_{\max}) = (-\infty, +\infty)$, the zeroth-order term $F_y^{(0)}$ vanishes: for symmetry reasons, there can be no net force on a planet sitting on corotation. The evaluation of the net force therefore requires the evaluation of the first-order term $F_y^{(1)}$. However, it is interesting to evaluate the zeroth-order term when the limits of integration are $(x_{\min}, x_{\max}) = (0, +\infty)$, i.e. when we consider the force exerted exclusively by the material outside corotation. Not only does that provide one of the solutions required to evaluate the net force ($\tilde{\rho}^{(0)}$), it also provides some insight into the disc response. Using a terminology similar to the one employed for Lindblad torques, we call this force the one-sided thermal force.

3.3 One-sided thermal force

As described in the previous section, we seek here the density response of the disc to the heating term:

$$\tilde{\mathcal{S}}^{(0)} = L\delta(x) = Lk\delta(X). \quad (74)$$

We call $[R_K(X), I_K(X)]$ the solution of the differential system of Eqs. (65) and (66) in which the forcing term is Dirac's distribution with a unitary weight:

$$X I_K = K(R_K'' - R_K) + \delta(X) \quad (75)$$

$$-X R_K = K(I_K'' - I_K), \quad (76)$$

and which satisfies $R_K(X) \rightarrow 0$ and $I_K(X) \rightarrow 0$ when $X \rightarrow \pm\infty$. We can obtain $R_K(X)$ and $I_K(X)$ with a shooting method, as presented in Appendix A. We have

$$\tilde{\rho}_R^{(0)}(X) = s R_K(X) \quad (77)$$

$$\tilde{\rho}_I^{(0)}(X) = s I_K(X), \quad (78)$$

with

$$s = -\frac{(\gamma-1)k^2 L}{q\Omega_p k_y c_s^2} \quad (79)$$

Using Eqs. (40), (64), (72), (78) and (79), we write the force exerted by the gas at $x > 0$ as

$$F_y^{\text{one-sided}} = \int_0^\infty \int_0^\infty f_y(k_y, k_z) dk_y dk_z, \quad (80)$$

where the force density in Fourier space $f_y(k_y, k_z)$ is given by

$$f_y(k_y, k_z) = \frac{2(\gamma-1)GML}{\pi q\Omega_p c_s^2} \int_0^\infty \exp(-X) I_K(X) dX. \quad (81)$$

The integral of the right-hand side is a real function of the variable K . We call it $F(K)$. Therefore, the one-sided force reads

$$F_y^{\text{one-sided}} = \frac{2(\gamma-1)GML}{\pi q\Omega_p c_s^2} \int_0^\infty \int_0^\infty F(K) dk_y dk_z. \quad (82)$$

We introduce the characteristic spatial frequency k_c as

$$k_c = \sqrt{\frac{q\Omega_p \gamma}{\chi}}, \quad (83)$$

and the dimensionless form of the wave vectors k_y and k_z as

$$K_y = k_y/k_c, \quad (84)$$

$$K_z = k_z/k_c. \quad (85)$$

Eq. (63) becomes

$$K = \frac{(K_y^2 + K_z^2)^{3/2}}{K_y}, \quad (86)$$

and we rewrite Eq. (82) as

$$F_y^{\text{one-sided}} = \frac{2(\gamma-1)GML}{\pi q \Omega_p c_s^2} k_c^2 \int_0^\infty \int_0^\infty F \left[\frac{(K_y^2 + K_z^2)^{3/2}}{K_y} \right] dK_y dK_z \quad (87)$$

The double integral can be recast into separable form using the variables (α, θ) such that

$$K_y = \alpha \sin \theta \quad (88)$$

$$K_z = \alpha \cos \theta. \quad (89)$$

We eventually obtain an expression involving a single integral only:

$$F_y^{\text{one-sided}} = \frac{\gamma(\gamma-1)GML}{\pi \chi c_s^2} \int_0^\infty F(\alpha) d\alpha. \quad (90)$$

Details about the numerical evaluation of this integral are given in Appendix B. We find

$$\int_0^\infty F(\alpha) d\alpha \approx 0.205, \quad (91)$$

so that

$$F_y^{\text{one-sided}} = \frac{0.0653\gamma(\gamma-1)GML}{\chi c_s^2}. \quad (92)$$

This force has the same dependence on the different physical parameters as the heating force worked out by [Masset & Velasco Romero \(2017\)](#) in a medium without shear, albeit with a markedly different numerical coefficient. Remarkably, it does not depend on the amount of shear q . This force is positive: the disturbance, which corresponds to a heated region with negative perturbation of density, tends to be displaced towards negative values of y by the Keplerian flow, and ultimately exerts a positive force on the planet.

3.4 Net thermal force

The thermal force exerted by the whole material, corresponding to Eqs. (71)-(73) with $(x_{\min}, x_{\max}) = (-\infty, +\infty)$, requires the evaluation of $\tilde{\rho}_I^{(1)}$. This quantity is given by the solution of the differential system of Eqs. (65) and (66) with the forcing term $\tilde{S}_p^{(1)}$ of Eq. (45)

$$\mathcal{S}_p^{(1)}(x) = -L\delta'(x) = -Lk^2\delta'(X). \quad (93)$$

We call $[r_K(X), i_K(X)]$ the solution of Eqs. (65)-(66) in which the forcing term is the negative of the derivative of Dirac's distribution with unitary weight:

$$Xi_K = K(r_K'' - r_K) - \delta'(X) \quad (94)$$

$$-Xr_K = K(i_K'' - i_K), \quad (95)$$

which satisfies the boundary condition $r_K(X), i_K(X) \rightarrow 0$ when $X \rightarrow \pm\infty$. From Eqs. (65), (66) and (93) we infer

$$\tilde{\rho}_I^{(1)} = -\frac{(\gamma-1)k^3L}{q\Omega_p k_y c_s^2} i_K(X). \quad (96)$$

Denoting with $F_y^{(1a)}$ the first part of the integral of Eq. (73)

$$F_y^{(1a)} = \frac{1}{\pi^2} \int_{-\infty}^{+\infty} dx \iint_{k_y>0, k_z>0} dk_y dk_z k_y \tilde{\Phi}_p^{(0)} \tilde{\rho}_I^{(1)}, \quad (97)$$

we have, using Eqs. (40), (64) and (96):

$$F_y^{(1a)} = \int_0^\infty \int_0^\infty f_y^{(1a)}(k_y, k_z) dk_y dk_z, \quad (98)$$

with

$$f_y^{(1a)}(k_y, k_z) = \frac{4(\gamma-1)kGML}{\pi q \Omega_p c_s^2} \int_0^\infty \exp(-X) i_K(X) dX. \quad (99)$$

The integral of the right-hand side is a function of the variable K , that we call $J(K)$. Note that we have an extra factor of 2 in Eq. (99) because the integration is now performed over the whole disc, and we have used the fact that $\tilde{\rho}_I^{(1)}$, or $i_K(X)$, are even functions of X . We have, using Eqs. (84)-(86) and (99)

$$F_y^{(1a)} = \frac{4(\gamma-1)GML}{\pi q \Omega_p c_s^2} k_c^3 \times \int_0^\infty \int_0^\infty (K_y^2 + K_z^2)^{1/2} J \left[\frac{(K_y^2 + K_z^2)^{3/2}}{K_y} \right] dK_y dK_z. \quad (100)$$

Using again the variables of Eqs. (88)-(89) and Eq. (83), we obtain

$$F_y^{(1a)} = \frac{4(\gamma-1)GML}{3\pi q \Omega_p c_s^2} k_c^3 \int_0^\infty J(\alpha^{2/3}) d\alpha \int_0^{\pi/2} \sin^{3/2} \theta d\theta \approx \frac{0.371\gamma^{3/2}(\gamma-1)GMLq^{1/2}\Omega_p^{1/2}}{\chi^{3/2}c_s^2} \int_0^\infty J(\alpha^{2/3}) d\alpha \quad (101)$$

We give in Appendix B details about the evaluation of the integral of Eq. (101). We find

$$\int_0^\infty J(\alpha^{2/3}) d\alpha \approx 0.616, \quad (102)$$

and thus

$$F_y^{(1a)} \approx \frac{0.228\gamma^{3/2}(\gamma-1)GMLq^{1/2}\Omega_p^{1/2}}{\chi^{3/2}c_s^2} \quad (103)$$

We now turn to the second part of Eq. (73), that we call $F_y^{(1b)}$:

$$F_y^{(1b)} = \frac{1}{\pi^2} \int_{-\infty}^{+\infty} dx \iint_{k_y>0, k_z>0} dk_y dk_z k_y \tilde{\Phi}_p^{(1)} \tilde{\rho}_I^{(0)}. \quad (104)$$

Using Eqs. (41), (78) and (79), we can write

$$F_y^{(1b)} = \int_0^\infty \int_0^\infty f_y^{(1b)}(k_y, k_z) dk_y dk_z, \quad (105)$$

with

$$f_y^{(1b)} = \frac{4(\gamma-1)kGML}{\pi q \Omega_p c_s^2} F(K). \quad (106)$$

The form $f_y^{(1b)}$ is very similar to that of $f_y^{(1a)}$, except that it features $F(K)$ instead of $J(K)$. We can therefore directly write

$$F_y^{(1b)} \approx \frac{0.371\gamma^{3/2}(\gamma-1)GMLq^{1/2}\Omega_p^{1/2}}{\chi^{3/2}c_s^2} \int_0^\infty F(\alpha^{2/3})d\alpha. \quad (107)$$

An approximate numerical value of the integral (see Appendix B) is 0.252. Not surprisingly, $F_y^{(1a)}$ and $F_y^{(1b)}$ have a positive sign. The former, because the force exerted at the origin by the disturbance excited by a planet at $x_p > 0$ is positive, as the outer disc receives more heat (we have seen that the outer disc exerts a positive force on a mass located at the origin), and the latter because the force exerted at the location $(x, 0, 0)$ (with $x > 0$) by the disturbance excited by a planet located at the origin is positive, since this location is closer from the disturbance of the outer disc.

We eventually have

$$F_y^{(1)} = F_y^{(1a)} + F_y^{(1b)} \approx \frac{0.322\gamma^{3/2}(\gamma-1)GMLq^{1/2}\Omega_p^{1/2}}{\chi^{3/2}c_s^2} \quad (108)$$

and the net thermal force is

$$F_y = x_p F_y^{(1)} \approx \frac{0.322x_p\gamma^{3/2}(\gamma-1)GMLq^{1/2}\Omega_p^{1/2}}{\chi^{3/2}c_s^2}. \quad (109)$$

Unlike the one-sided thermal force, the net force does depend on the shear. It also has a steeper dependence on the thermal diffusivity than the one-sided force, and it has the same sign as x_p , for the reasons explained above.

3.5 Response in real space

It is instructive to examine the form of the response in real space. Denoting with a hat the one-dimensional Fourier transform in z , we have

$$\hat{\rho}(x, y, k_z) = \int_{-\infty}^{+\infty} \rho'(x, y, z) e^{-ik_z z} dz \quad (110)$$

and

$$\hat{\rho}(x, y, k_z) = \frac{1}{2\pi} \int_{-\infty}^{+\infty} \tilde{\rho}(x, k_y, k_z) e^{ik_y y} dk_y \quad (111)$$

The perturbation of surface density $\Sigma'(x, y)$ is also $\hat{\rho}(x, y, 0)$. We introduce the reduced coordinates $x' = x/k_c$ and $y' = y/k_c$, and the perturbation of surface density σ' as a function of (x', y')

$$\sigma'(x', y') = \Sigma'(x'/k_c, y'/k_c). \quad (112)$$

We have

$$\sigma'(x', y') = \frac{1}{2\pi} \int_{-\infty}^{+\infty} \tilde{\rho}(x'/k_c, k_y, 0) e^{ik_y y'/k_c} dk_y. \quad (113)$$

We can write the first-order expansion of $\sigma'(x', y')$ in x_p , using the decomposition of section 2.3. We have

$$\sigma'(x', y') = \sigma'^{(0)}(x', y') + x_p \sigma'^{(1)}(x', y') + \mathcal{O}(x_p^2), \quad (114)$$

where $\sigma'^{(i)}$ is obtained substituting $\tilde{\rho}$ by $\tilde{\rho}^{(i)}$ in Eq. (113). Noting from Eqs. (63), (79) and (83) that for $k_z = 0$, we have

$$K = k_y |k_y| / k_c^2 \quad (115)$$

and

$$\tilde{\rho}^{(0)}(x'/k_c, k_y, 0) = s [R_K(x'k_y/k_c) + iI_K(x'k_y/k_c)] \quad (116)$$

with

$$s = -\frac{\gamma(\gamma-1)L}{\chi c_s^2} \times \frac{k_y}{k_c^2}, \quad (117)$$

we have

$$\begin{aligned} \sigma'^{(0)}(x', y') &= -\frac{\gamma(\gamma-1)L}{\pi \chi c_s^2} \\ &\times \int_0^\infty K_y [R_{K_y^2}(x'K_y) \cos(y'K_y) - I_{K_y^2}(x'K_y) \sin(y'K_y)] dK_y, \end{aligned} \quad (118)$$

where we have used Eq. (84). In a similar fashion, using Eq. (96), we obtain

$$\begin{aligned} \sigma'^{(1)}(x', y') &= -\frac{\gamma(\gamma-1)Lk_c}{\pi \chi c_s^2} \\ &\times \int_0^\infty K_y^2 [r_{K_y^2}(x'K_y) \cos(y'K_y) - i_{K_y^2}(x'K_y) \sin(y'K_y)] dK_y, \end{aligned} \quad (119)$$

where we have used the parity in K of the functions R_K , r_K , I_K and i_K to integrate over positive values of K_y (the first two are odd in K , while the other two are even in K). These relations show that the perturbation of surface density by a planet at the origin, and its derivative with respect to the planet's distance to corotation, are universal maps of the normalized coordinates, and that they are proportional to the factors in front of the integrals. The scaling factor k_c is the same for the x - and y -coordinates, which implies that the shape of the planet's response is independent of the shear and of the thermal diffusivity. Changing one of these parameters changes the size of the disturbance, but not its aspect ratio. Fig. 1 shows the aspect of $\sigma'^{(0)}$ and $\sigma'^{(1)}$.

3.6 Physical picture

The physical picture that emerges from the previous sections is that the heat released by a luminous planet into its surroundings yields a low-density region, over a length-scale

$$\lambda_c = k_c^{-1} = \sqrt{\chi/q\Omega_p\gamma}, \quad (120)$$

which is distorted by the Keplerian shear. When the planet is centred on corotation ($x_p = 0$), no net force is exerted, for symmetry reasons. In this situation, the outer and inner lobes exert opposite forces of magnitude $F_y^{\text{one-sided}} \sim GML/\chi c_s^2$ (we discard occurrences of the adiabatic index and numerical factors in this discussion on orders of magnitude). When the planet is away from corotation, the symmetry is broken and it experiences a net force of magnitude $F_y \sim (x_p/\lambda_c) F_y^{\text{one-sided}}$. Although our expansion is valid for $|x_p| \ll \lambda_c$, we can estimate the magnitude of the net force when the distance to corotation becomes comparable to or larger than λ_c . Masset & Velasco Romero (2017) have evaluated the force arising from the release of heat by a perturber in a homogeneous medium without shear. They showed that the response time of the force, in the regime of low Mach numbers, is $\tau \sim \chi/V^2$, where V is the velocity of

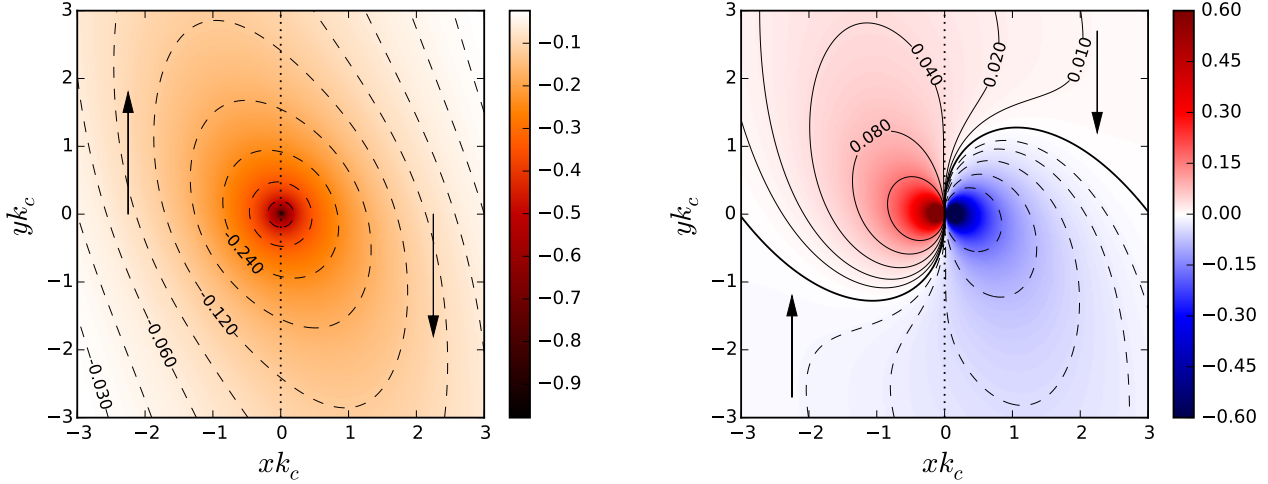


Figure 1. Perturbation of surface density $\sigma^{(0)}$ in units of $\gamma(\gamma-1)L/\chi c_s^2$ due to the singular heat release $L\delta(r)$ (left) and perturbation $\sigma^{(1)}$ arising from the heat ‘dipole’ $-L\delta'(x)\delta(y)\delta(z)$, in units of $\gamma(\gamma-1)Lk_c/\chi c_s^2$ (right). The map of the right can also be regarded as the derivative of the perturbation of surface density with respect to the planet position x_p . These maps have been obtained by summing 40 000 Fourier components in geometric sequence from $k_y = 10^{-4}k_c$ to $k_y = 10^4k_c$. The levels on the left map are in geometric sequence with a ratio of $\sqrt{2}$ from -3×10^{-2} to -0.48 , while the levels on the right map are in geometric sequence with a ratio of 2 from $\pm 1 \times 10^{-2}$ to ± 0.16 . The thicker contour corresponds to the null level. The vertical arrows depict schematically the Keplerian flow. When the distance to the planet is largely smaller than λ_c (i.e. for $|xk_c| \ll 1$ and $|yk_c| \ll 1$), diffusion dominates and the perturbation has spherical symmetry. For distances comparable to or larger than λ_c , advection takes over and the perturbation is distorted under the action of the Keplerian flow.

the perturber with respect to the gas. In the present situation, when the response time is shorter than the time-scale of the shear $(q\Omega_p)^{-1}$, the shear is unimportant and the net force on the perturber can be approximated by the expression of [Masset & Velasco Romero](#). This occurs when

$$\frac{\chi}{(q\Omega_p x_p)^2} \lesssim \frac{1}{q\Omega_p} \quad (121)$$

or equivalently when $x_p \gtrsim \lambda_c$. The length-scale λ_c is therefore also the distance to corotation beyond which the shear becomes irrelevant. When the planet’s distance to corotation is larger than λ_c , the force tends towards the value $\sim GML/(\chi c_s^2)$ ([Masset & Velasco Romero 2017](#)). When it is much smaller than λ_c , it obeys the linear scaling given by Eq. (109). We note that Eq. (109) evaluated for $x_p = \lambda_c$ gives approximately 2/3 of the value given by [Masset & Velasco Romero \(2017\)](#).

4 COLD PLANET

We now turn to the case of a non-luminous planet. We denote with an index a the perturbations of the different hydrodynamics quantities when the disc is adiabatic ($\chi = 0$), and with an index t the difference between the solution with a finite thermal diffusivity and the solution of the adiabatic case. Hence, by definition, we can write

$$\tilde{\rho} = \tilde{\rho}_a + \tilde{\rho}_t, \quad (122)$$

$$\tilde{p} = \tilde{p}_a + \tilde{p}_t. \quad (123)$$

In this whole section, we do not write an index Φ for the different hydrodynamics variables in order to improve legibility, but it must be understood that they are components

of Q_Φ , i.e. of the disc’s response to a perturber with non-vanishing gravitational potential and with $L = 0$.

Eq. (28) implies that when the disc is adiabatic ($\chi = 0$) and the planet is non-luminous ($\tilde{S}_p = 0$):

$$\tilde{p}_a - c_s^2 \tilde{\rho}_a = 0. \quad (124)$$

When $\chi \neq 0$ (and $\tilde{S}_p = 0$), Eq. (28) can be rewritten as:

$$-iqk_y \Omega_p x (\tilde{p}_t - c_s^2 \tilde{\rho}_t) - \chi \Delta' \left(\tilde{p}_t - \frac{c_s^2}{\gamma} \tilde{\rho}_t \right) = \chi \Delta' \left(\tilde{p}_a - \frac{c_s^2}{\gamma} \tilde{\rho}_a \right), \quad (125)$$

Using Eq. (124), we can simplify the right-hand side and obtain:

$$-iqk_y \Omega_p x (\tilde{p}_t - c_s^2 \tilde{\rho}_t) - \chi \Delta' \left(\tilde{p}_t - \frac{c_s^2}{\gamma} \tilde{\rho}_t \right) = \frac{\gamma-1}{\gamma} \chi \Delta' \tilde{p}_a. \quad (126)$$

The additional perturbation of density $\tilde{\rho}_t$ arising from a finite thermal diffusivity obeys therefore an equation similar to Eq. (28), in which $(\gamma-1)/\gamma \cdot \chi \Delta' \tilde{p}_a$ plays the role of the heat source.

Using Eq. (33), we can write

$$\tilde{\rho}_a = \mathcal{L} \left(\Phi_p + \frac{\tilde{p}_a}{\rho_0} \right) \quad \text{and} \quad \tilde{\rho} = \mathcal{L} \left(\Phi_p + \frac{\tilde{p}}{\rho_0} \right). \quad (127)$$

We note that the thermal diffusivity χ does not feature in the expression of the operator \mathcal{L} , so that it has same expression in the two instances of the above identities. The linearity of this operator implies

$$\tilde{\rho}_t = \mathcal{L} \left(\frac{\tilde{p}_t}{\rho_0} \right). \quad (128)$$

Therefore, as shown in section 2.2, the relative perturbation

of pressure arising from the finite thermal diffusion is negligible compared to that of density: $|\tilde{p}_t/\rho_0| \ll |\tilde{\rho}_t/\rho_0|$, which allows us to simplify Eq. (126) into

$$iqk_y\gamma\Omega_p x\tilde{\rho}_t + \chi\Delta'\tilde{\rho}_t = \frac{\gamma-1}{c_s^2}\chi\Delta'\tilde{p}_a. \quad (129)$$

Eq. (129) is considerably more complex than the equation (58) for a luminous planet that we solved in section 3, in which the source terms of heat were singular at the origin. The source term in $\Delta'\tilde{p}_a$ has here a complex structure over the whole wake triggered by the planet in an adiabatic disc. It has, however, a nearly singular component at the planet's location, as we shall see below. We are going to restrict ourselves to the study of this particular component, and to the force or torque it exerts on the planet. How a finite thermal diffusivity further affects the torque will be discussed in section 5.4, but is not studied in detail in this work.

We use the fact that the response of an adiabatic disc in the immediate vicinity of a low, sub-thermal mass planet (i.e. at distances shorter than the pressure length-scale) is such that the planetary potential well is almost filled with enthalpy, so that the distribution of the gas near the planet resembles that of an isentropic atmosphere in hydrostatic equilibrium. We discuss the validity of this assumption in Appendix C. We therefore use the approximate relationship

$$\rho_0\Phi_p + p'_a = 0 \quad (130)$$

to continue our calculation. Using Poisson's equation, we arrive at

$$iqk_y\Omega_p x\tilde{\rho}_t + \frac{\chi}{\gamma}\Delta'\tilde{\rho}_t = -\frac{4\pi GM\chi\rho_0(\gamma-1)}{c_s^2\gamma}\delta(x-x_p), \quad (131)$$

where we have made the approximation $\Delta(-\rho_0\Phi_p) \approx -\rho_0\Delta\Phi_p$, that we justify in Appendix D. The density perturbation arising from a finite thermal diffusivity is formally similar to the density perturbation $\tilde{\rho}_H$ arising from a singular heat release by the planet, given by Eq. (58), with the negative luminosity $-L_c$, where L_c is given by

$$L_c = \frac{4\pi GM\chi\rho_0}{\gamma}. \quad (132)$$

All the results found in section 3 can be applied directly, except for a change of sign. Instead of two hot, low-density lobes, we have here two cold, dense lobes on either side of corotation. The one-sided force arising from any of these lobes has a familiar value. Using Eqs. (92) and (132), we find

$$\left|F_y^{\text{one sided, cold}}\right| = \frac{0.821(\gamma-1)G^2M^2\rho_0}{c_s^2} \quad (133)$$

This quantity might be easier to recognize if we use the relationships $\rho_0 = \Sigma/\sqrt{2\pi}H$, $c_s^2 = \gamma H^2\Omega_p^2$ and write the torque $\Gamma = r_p F_y$ in terms of Γ_0 defined by

$$\Gamma_0 = \Sigma r_p^4 \Omega_p^2 \mu^2 h^{-3}, \quad (134)$$

where $h = H/r_p$ is the disc's aspect ratio and $\mu = M/M_\star$. We obtain

$$\left|\Gamma_{\text{thermal}}^{\text{one sided, cold}}\right| = 0.33 \frac{\gamma-1}{\gamma} \Gamma_0 \quad (135)$$

To within a dimensionless factor, this is the one-sided Lindblad torque² (Ward 1997). The cold thermal lobes therefore exert on the planet torques comparable in magnitude to the wake's torques. The analogy even holds for the signs: the outer lobe exerts a negative torque on the planet, as does the wake of the outer disc, while the opposite holds for the inner disc.

The net thermal force can be derived using Eqs. (109), (132) and (134). We obtain:

$$\Gamma_{\text{thermal}}^{\text{cold}} = -1.61 \frac{\gamma-1}{\gamma} \frac{x_p}{\lambda_c} \Gamma_0. \quad (136)$$

In Eqs. (133) and (136) we have used the subscript *thermal* to indicate that these torque components arise from $\tilde{\rho}_t$, and must be added to the torque arising from $\tilde{\rho}_a$ (i.e. the torque exerted on the planet in an adiabatic disc) to get the total torque acting on the planet.

5 DISCUSSION

We have worked out in section 3 the torque arising from the perturbation \mathbf{Q}_H , while in section 4 we have given an estimate of the torque increment arising from a finite thermal diffusivity, with respect to the adiabatic case. Both torques arise from the same physical process, that of the diffusion of heat and its advection by the Keplerian flow, over a distance typically shorter than the disc's pressure length-scale. We give them the generic name of thermal torques. More specifically, we keep for the former the name 'heating torque' used by Benítez-Llambay et al. (2015), and we call the latter the 'cold thermal torque' since it does not involve the release of heat by the planet. When the planet has a finite luminosity, the total thermal torque is the sum of the heating torque and of the cold thermal torque.

5.1 Comparison of the cold thermal torque and differential Lindblad torque

We have seen in the previous section that the one-sided Lindblad and thermal torques have the same order of magnitude. Which of the net torque (Lindblad or thermal) is larger therefore depends on the degree of asymmetry of each torque, as depicted in Fig. 2. An exploration of the parameter space being far beyond the scope of this work, we will fix ideas using the recent disc models of Bitsch et al. (2015). Namely we will use the same samples of these models as those considered by Masset & Velasco Romero (2017, in their table 1). These two samples correspond to the physical parameters in a *bona fide* protoplanetary disc at $r = 3$ au (hence at distances where planetary formation is supposed to take place) at two different dates: when the disc is young ($t = 300$ kyr) and when it is more evolved ($t = 1$ Myr) and has experienced a significant drop of temperature.

The ratio of the thermal torque to the Lindblad plus corotation torque scales with the ratio

$$\frac{x_p}{\lambda_c h} = \eta \frac{H}{\lambda_c} \quad (137)$$

² The one-sided Lindblad torque depends on the disc profile, and is typically $\sim \Gamma_0/2$.

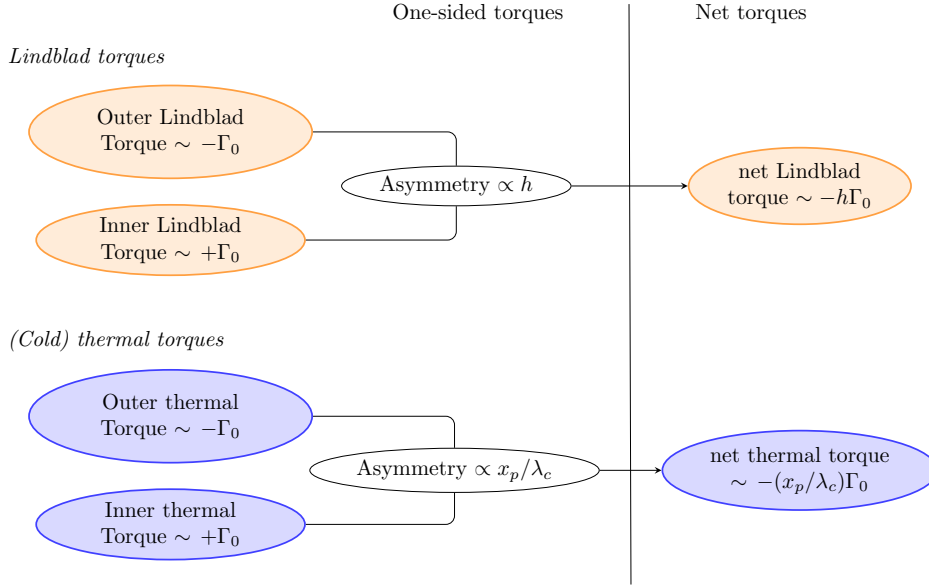


Figure 2. Schematic comparison between the Lindblad torque and the cold thermal torque. The net (or differential) Lindblad torque arises from an asymmetry of the one-sided Lindblad torques. The residual value is of order $-h\Gamma_0$, as it is the length-scale of pressure that sets the asymmetry between the torques at inner and outer Lindblad resonances. The corotation torque, not shown here, has same scaling, with a dimensionless coefficient different from that of the differential Lindblad torque, which depends on the disc’s profile. Similarly, the net thermal torque arises because of an asymmetry between the outer and inner one-sided thermal torques. The amount of asymmetry, and the ultimate value of the net thermal torque, depends on the ratio of the corotation offset x_p to the size of the thermal lobes λ_c . Assessing which of the two kinds of torque is stronger (Lindblad plus corotation, or thermal torque) therefore amounts to comparing x_p/λ_c to h .

where we have used the relation

$$x_p = \eta h^2 r_p, \quad (138)$$

η being a dimensionless coefficient of order unity that depends on the profiles of surface density and temperature. The torque ratio therefore scales with the ratio of the pressure length-scale (or disc’s thickness) to the size of the thermal disturbance. We have assumed this ratio to be large in our derivation. For the first disc model that we consider (left column of table 1 of [Masset & Velasco Romero](#)), the ratio H/λ_c is ~ 4.8 , whereas for the second disc model it has the value ~ 12 . This essentially validates the key assumption made in section 2.1 that $\lambda_c \ll H$.

We can make more quantitative the comparison between the Lindblad plus corotation torque and the cold thermal torque by taking into account the dimensionless factors of order unity. When the surface density and temperature profiles are power laws of the radius (respectively with exponents $-\alpha$ and $-\beta$), one has, using Eq. (12)

$$\eta = \frac{\alpha}{3} + \frac{\beta + 3}{6}. \quad (139)$$

In the disc models that we consider, in which $(\alpha, \beta) \approx (1/2, 1)$ for the first model and $(\alpha, \beta) \approx (0, 1)$ for the second model, we have respectively $\eta \approx 0.8$ and $\eta \approx 0.7$. Specialising, from now on, to the case $\gamma = 7/5$, adequate for protoplanetary discs, we get from Eq. (136):

$$\begin{aligned} \Gamma_{\text{thermal}}^{\text{cold}} &\approx -1.8h\Gamma_0 \quad \text{for model 1,} \\ \Gamma_{\text{thermal}}^{\text{cold}} &\approx -3.9h\Gamma_0 \quad \text{for model 2.} \end{aligned}$$

These estimates are to be compared with the typical value

of the Lindblad plus corotation torque³, which is generally in the range $[-2h\Gamma_0/\gamma, 2h\Gamma_0/\gamma]$ (see e.g. [Lega et al. 2015](#); [Jiménez & Masset 2017](#)), and rather on the lower side of this interval for planets of the order of one to a few Earth masses.

This indicates that for protoplanets or planetary embryos with a mass sufficiently small to be subjected to the thermal torque, the latter is an essential component of the total torque. In particular, in discs with low thermal diffusivity (as the disc model 2), the thermal torque can be so large that it makes the Lindblad and corotation torques virtually irrelevant. Since the thermal torque scales with the offset to corotation x_p , embryos mainly driven by the thermal torque should be trapped at or near the pressure traps (locations where the pressure gradient, and therefore the offset to corotation, cancel out) much as lower mass objects driven by aerodynamic drag.

5.2 Critical mass for heat release

The planetary mass up to which thermal torques are significant is an open question. In the context of dynamical friction, [Masset & Velasco Romero \(2017\)](#) argue that the

³ We warn the reader against a possible confusion between our definition of Γ_0 , which scales as h^{-3} as does the one-sided Lindblad torque, and the definition adopted in many publications, which involves h^{-2} rather than h^{-3} , and which corresponds to the scaling of the differential Lindblad or corotation torques. This is why in the present work the net Lindblad or corotation torque scales with $h\Gamma_0$ rather than Γ_0 .

estimate of the heating force obtained by a linear analysis holds when the heat released by the planet entirely ends up as an excess of internal energy outside of the Bondi sphere⁴. This occurs when the time-scale for heat diffusion across Bondi's radius $r_B = GM/c_s^2$ is shorter than the acoustic time r_B/c_s . This condition translates into $M < M_c = \chi c_s/G$. For masses larger than this critical value, it is not guaranteed that the internal energy injected in the gas near the planet emerges as an excess of internal energy outside of the Bondi sphere, and one may expect a cut-off of the thermal force.

The exploration of the parameter space of Benítez-Llambay et al. (2015), which shows a cut-off of the heating torque above a few Earth masses, is compatible with this expectation. Similarly, the work of Lega et al. (2014), which is likely the only numerical evidence of the cold thermal torque to date (as we shall see in section 5.3.1), shows that this effect vanishes past $\sim 3M_\oplus$. This set of evidence is rather slim, however, and a thorough study of the thermal torques as a function of the planetary mass is necessary to provide useful formulae that can be incorporated to models of planetary population synthesis. Owing to the non-linear nature of the flow within the Bondi sphere, a systematic study of the mass dependence may need to resort to numerical simulations. There is nevertheless a foreseeable difficulty inherent to such study. The mass range of interest and the resolution requirements are such that the time step of an explicit scheme will not be limited by the sound speed, but necessarily by heat diffusion, potentially yielding very short time steps. Unless heat diffusion is dealt with in an implicit manner, or accelerated by the use of a super time-stepping technique (Alexiades et al. 1996), the calculations may prove impracticable.

We also note that even in the barotropic case complex phenomena occur in the Bondi sphere of a low-mass planet (Fung et al. 2015; Ormel et al. 2015a,b; Fung et al. 2017). In the particular case in which the gas is isothermal, there is a large mass build-up within the Bondi sphere owing to the lack of compressional heating, with potentially a large impact on the torque (Fung et al. 2015). For sub-critical planets ($M < M_c$), the flow may be considered as nearly isothermal within the Bondi sphere. The enhancement of density ρ_t experienced in such case by a cold planet leads to a similar mass build up as in the isothermal case, which may have an impact on the torque. The investigation of this highly non-linear small-scale flow is largely beyond the scope of this work. It likely requires to be tackled by means of numerical simulations. While the Bondi sphere of nearly thermal-mass planets ($\mu \sim h^3$) can be resolved on modern computational platform, that of deeply embedded objects ($\mu \ll h^3$) such as those considered here cannot be resolved with present-day computational resources (Fung et al. 2015), at least for global disc simulations.

Until a detailed exploration of the thermal effects that resolves the flow at the sub-Bondi scale and provides the magnitude of the force as a function of the planetary mass is available, we caution that estimates of the thermal torques should be valid only when $M < M_c$, and regarded as upper values otherwise.

5.3 Comparison to earlier work

5.3.1 Cold thermal torque and the 'cold finger' effect

The cold thermal torque has been quite elusive so far in numerical simulations of embedded protoplanets. There are several reasons for that: (i) it requires a finite thermal diffusivity of the gas, while the vast majority of the numerical studies used either isothermal or adiabatic setups; (ii) a finite thermal diffusivity is generally achieved through the use of some sort of radiative transfer (such as flux limited diffusion), which considerably increases the numerical cost over what could be achieved if thermal diffusion was modelled as in the present work, and consequently decreases the size of the parameter space that can be explored, (iii) thermal torques are exerted on low or very low mass planets (up to a few Earth masses at most), which are not systematically included in studies of planet-disc interactions with radiative transfer and (iv) the thermal lobes are typically an order of magnitude smaller than the length-scale of pressure, and are barely captured even with state-of-the-art resolutions. To the knowledge of the author, there is only one mention in the literature of the effect that we described here as the cold thermal torque: Lega et al. (2014) found that Earth-sized planets in 3D radiative discs were subjected to a negative torque which could be accounted for neither by the Lindblad torque nor by the corotation torque. The radial density of the torque shows strong contributions bound to the coorbital region, negative outside and positive inside, with a marked asymmetry in favour of the outside component. All of these features are compatible with the effect we report here. One can furthermore estimate the thermal diffusivity at the midplane of the disc considered by these authors to be $\chi \approx 1.5 \times 10^{15} \text{ cm}^2\text{s}^{-1}$, from which we can estimate, for their planets orbiting a solar mass star at $r_p = 5.2 \text{ au}$, that $\lambda_c = 0.014 \text{ au}$, compatible with the extent of the peaks found in their radial torque distribution. Incidentally, this shows that in their disc, they have $H/\lambda_c \approx 14$, bringing further evidence that the thermal lobes are in general much smaller than the pressure length-scale. We can also estimate the corotation offset x_p , in their setup, to be of the order of $6 \times 10^{-3} \text{ au}$, which represents a fair fraction of λ_c , the characteristic size of the thermal lobes, and can account for the strong asymmetry between the inner and outer torques. Finally, they observe a strong difference in the torque distribution between their lightest planet (with mass $2M_\oplus$) and the next one (with mass $3M_\oplus$), indicating that the effect is probably already cut-off in their simulations, at least above the lowest mass considered. As further evidence to support this claim, we note that Eq. (136) predicts a cold thermal torque of the order of $-5.5h\Gamma_0$, which would result in a total torque much larger in absolute value than the values they report even for $2M_\oplus$, which seems to indicate that even for this lowest mass the effect is already significantly cut-off. We comment however that this discrepancy can also be attributed, at least partially, to the low resolution with which the lobes are captured.

These authors reported their effect as the formation of 'cold fingers'. This denomination likely arises from subsequent two-dimensional simulations that they perform, in which the cooling of fluid parcels is not due to heat diffusion but to an exponential relaxation towards a prescribed

⁴ If the luminosity is not too large, the Bondi sphere encloses the region where the flow is non-linear.

equilibrium temperature, resulting in a larger entropy loss for gas parcels that experience more compressional heating. This numerical experiment is enlightening as it explains the formation of cold, dense structures past the planet. The resulting disturbances, nonetheless, do not arise from an advection-diffusion equation as the one we solved here, but merely from advection and cooling, which results in much more narrow, elongated features. We suggest that the denomination ‘cold lobes’ is more adequate when there is thermal diffusion.

5.3.2 Heating torque

The heating torque, analysed in section 3, has been studied by means of numerical simulations by Benítez-Llambay et al. (2015). Most of the remarks that we made for the work of Lega et al. (2014) in section 5.3.1 also apply to this work, except for a change of sign. Also, the disc’s thermal diffusivity in this work is approximately 2.9 times larger than that of Lega et al., which implies that the length-scale λ_c of the thermal lobes is 1.7 times larger (the distance to the central star, and the mass of the latter, are the same in both works). This is compatible with the radial torque density presented by Benítez-Llambay et al. (2015). We mention that their ‘neutral run’, in which the heat release is disabled, does include a cold thermal torque. The planet’s luminosity in the fiducial calculation of this work is $L = 6.0 \times 10^{27}$ erg s⁻¹. Noting that Eq. (109) can be rewritten, using Eq. (138) as

$$\Gamma^{\text{heating}} = 0.261\eta \frac{GML}{(\chi\Omega_p)^{3/2}}, \quad (140)$$

and noting that here $\eta = 5/6$, we would predict for the heating torque a value of $\Gamma^{\text{heating}} \sim 2.7 \times 10^{36}$ g cm²s⁻². This value is typically one order of magnitude larger than the value measured. As for the simulations of Lega et al. (2014), this may constitute an indication that the thermal torques are cut-off. The discrepancy may also partly arise from the barely sufficient resolution (λ_c is just twice the radial resolution, and marginally smaller than the azimuthal resolution in that work).

The main trend found by Benítez-Llambay et al. (2015), which is a strong dependence on the disc’s opacity, is qualitatively compatible with the results of Eq. (109): the larger the opacity, the smaller the thermal diffusivity, and the larger the heating torque. The comparison cannot be made quantitative, however: the fiducial mass considered in this work is largely beyond the critical mass $\chi c_s/G$, and the latter furthermore varies when the opacity varies. They also find the heating torque to scale with the distance to corotation, which is compatible with our findings.

Finally, we mention that the luminosity L_c of Eq. (132) is $\sim 1.1 \times 10^{27}$ ergs s⁻¹, largely smaller than the luminosity of the fiducial run of Benítez-Llambay et al. (2015). It would correspond to a mass doubling time of ~ 500 kyr. The cold thermal torque has therefore only a mild impact in the runs of that work.

5.4 Additional effect of thermal diffusion on the torque

As mentioned in section 4, we have restricted ourselves, in the cold case, to the study of the disturbance triggered by

the singular component at the planet’s location. Yet, one may expect thermal diffusion to have a more direct, intuitive effect on the wake’s torque, if we omit the singular component: at low thermal diffusivity, the wake essentially behaves adiabatically and exerts the same torque as in an adiabatic disc, whereas at large thermal diffusivity it should behave isothermally and exert the same torque as in an isothermal disc. It is easy, however, to realize that the thermal diffusivity is usually sufficiently small for the wake’s torque to have the adiabatic value, when, as we noted in previous sections, $H \gg \lambda_c$. The exchange of angular momentum between the planet and the disc at a given Lindblad resonance occurs essentially over the first wavelength of the wave launched at the resonance. For waves with low azimuthal wavenumber m ($m < h^{-1}$), the wave vector of the disc’s response over the first wavelength is dominated by its radial component and has the order of magnitude $|k| \sim (m/h^2)^{1/3}/r_p$, whereas waves with large azimuthal wavenumber ($m > h$) have a wave vector dominated by its azimuthal component so that $|k| \sim m/r$. A wave with wave vector k and frequency ω behaves adiabatically if k is smaller than

$$k_{\text{cut}} = \sqrt{\omega/\chi} \quad (141)$$

The frequency of the waves launched at Lindblad resonances is the local epicyclic frequency, which is also close to Ω_p for a Keplerian disc. Waves with low azimuthal wavenumber therefore satisfy $k < (\lambda_c/H)k_{\text{cut}}$, and behave adiabatically. Waves with high azimuthal wavenumber will reach the cut-off wavenumber for $m \sim r/\lambda_c = (H/\lambda_c)h^{-1}$. This wavenumber is considerably larger than the wavenumber for the torque peak, which occurs for $m \sim h^{-1}/2$ (Ward 1997), so that virtually all resonances involved in the angular momentum exchange should excite an adiabatic response. From these arguments we also see that a transition towards another regime should be expected when $H \sim \lambda_c$, i.e. when $\chi \sim H^2\Omega_p$. This is the critical thermal diffusivity considered by Masset & Casoli (2010), who performed a fit of the Lindblad torque as a function of the thermal diffusivity. Alternatively, Paardekooper et al. (2011) use a one-dimensional wave model in a uniform medium as a guideline, and work out an effective adiabatic index γ_{eff} . They find a turnover diffusivity a factor of $\sim h$ smaller than $H^2\Omega_p$, as they consider the wave frequency in the inertial frame ($m\Omega_p$) rather than in the local frame. It is unclear what value one should expect for the Lindblad torque when χ becomes a sizeable fraction of $H^2\Omega_p$. In this regime, the waves launched at resonances are damped near their region of excitation. This process has been studied by Cassen & Woolum (1996) when thermal diffusion arises from radiative transfer. Although these issues definitely require further work, it should be clear that, for values of the thermal diffusivity typical of protoplanetary discs, they correspond to minute corrections to the torque, in comparison to the large effect of the cold thermal torque.

5.5 A simple expression for the total thermal torque

The total thermal torque is the sum of the heating torque and of the cold thermal torque:

$$\Gamma_{\text{thermal}}^{\text{total}} = \Gamma_{\text{thermal}}^{\text{heating}} + \Gamma_{\text{thermal}}^{\text{cold}} \quad (142)$$

while the total torque acting on the planet is

$$\Gamma^{\text{total}} = \Gamma_{\text{thermal}}^{\text{total}} + \Gamma_{\text{adiabatic}} \quad (143)$$

The heating torque given by Eq. (109) can be cast in a simple form using the critical luminosity L_c of Eq. (132). We obtain

$$\Gamma_{\text{thermal}}^{\text{heating}} = 1.61 \frac{\gamma - 1}{\gamma} \frac{x_p}{\lambda_c} \frac{L}{L_c} \Gamma_0, \quad (144)$$

while the total thermal torque is

$$\Gamma_{\text{thermal}}^{\text{total}} = 1.61 \frac{\gamma - 1}{\gamma} \frac{x_p}{\lambda_c} \left(\frac{L}{L_c} - 1 \right) \Gamma_0. \quad (145)$$

This expression can also be recast under the convenient form

$$\Gamma_{\text{thermal}}^{\text{total}} = 1.61 \frac{\gamma - 1}{\gamma} \eta \left(\frac{H}{\lambda_c} \right) \left(\frac{L}{L_c} - 1 \right) h \Gamma_0, \quad (146)$$

where η is given by Eq. (139), λ_c by Eq. (120), L_c by Eq. (132) and Γ_0 by Eq. (134).

5.6 Dependence on the disc gradients

The analysis presented in Sections 2-4 allows for a radial gradient of density, but assumes the background temperature to be uniform. The perturbation of density in the heated region does not depend on the background density [a similar result was obtained by [Masset & Velasco Romero \(2017\)](#) for the hot plume created by a hot body in a uniform medium]. This result holds as long as the perturbation of density is a small fraction of the unperturbed density. In the cold case, the perturbation of density does feature the unperturbed density at the planet's location. Therefore, no dependence of the thermal torques on the unperturbed density gradient should be expected, other than through the dependence on the corotation offset x_p .

We can estimate the dependence of the thermal torque on the temperature gradient as follows. A temperature gradient yields a correction that has the order of magnitude:

$$\Delta \beta \Gamma_{\text{thermal}} \sim \Gamma^{\text{one-sided}} c_s^2 \partial_r \left(\frac{1}{c_s^2} \right) \lambda_c = \beta \Gamma^{\text{one-sided}} \frac{\lambda_c}{r_p}. \quad (147)$$

We compare this correction to the thermal torque $\Gamma_{\text{thermal}} \sim (x_p/\lambda_c) \Gamma^{\text{one-sided}}$:

$$\left| \frac{\Delta \beta \Gamma_{\text{thermal}}}{\Gamma_{\text{thermal}}} \right| \sim |\beta| \frac{\lambda_c^2}{r_p x_p} \sim |\beta| \frac{\lambda_c^2}{H^2} \ll 1. \quad (148)$$

The correction is therefore negligible. Contrary to what happens for the case of the Lindblad torque, the region that exerts the torque is so compact that the gradient of background temperature does not have a sizeable impact on the torque value, and the thermal torques have no dependence on the temperature profile other than the one borne by the corotation offset x_p (see equations 138 and 139).

The torque expressions given in section 5.5 are therefore valid in discs with arbitrary surface density and temperature gradients.

5.7 On the negative luminosity of the cold case

The physical picture of the heating torque gives some insight into the mechanism of the cold thermal torque, which is very similar in nature. When the disc is adiabatic, there is a peak of temperature $T = p/\rho$ at the location of a non-luminous planet, since the potential well of the planet is almost topped off with enthalpy. The introduction of thermal diffusion flattens this peak over a distance $\sim \lambda_c$. As for the heating torque, this is achieved with perturbations of temperature and density of opposite signs, and virtually no perturbation of pressure. This situation is represented graphically in Fig. 3, which shows the perturbations of temperature and density at distances from the planet sufficiently small so that they can be regarded as having spherical symmetry. We see in this figure that the density perturbation associated with the finite thermal diffusivity seems to stem from a singular heat source with negative luminosity. At larger scale, in steady state, the perturbed density adopts the same pattern as the perturbed density associated with the heat release, with an opposite sign. This shows that the cold thermal torque and the heating torque are two slightly different versions of the same process of diffusion-advection.

The fact that the density perturbation associated with thermal diffusion seems to stem from a point-like source arises from a coincidence between two laws in R^{-1} : that of the planetary potential and that of diffusion in three dimensions around a point-like source⁵. This coincidence is not fortuitous: it simply arises from the fact that both processes are described by two formally similar Poisson's equations with a singular right-hand side. This coincidence does not hold in two dimensions, where the planetary potential is still represented by a R^{-1} law, whereas the perturbation of density arising from the heat release by a point-like source is solution of a two-dimensional Poisson's equation, with a divergence in $\log R$ in the vicinity of the perturber. In these circumstances, the perturbation of density arising from thermal diffusion near a cold planet cannot be regarded as originating from a point-like source. More generally, this underscores the need for three-dimensional calculations to reproduce correctly the properties of the thermal torques.

This mechanism (flattening of the temperature peak by thermal diffusion, which triggers a density perturbation similar to the one that would arise from a singular heat sink) should be valid every time a point-like mass moves at low Mach number within a non-adiabatic gas. Under these circumstances, thermal diffusion imparts a perturbation to the flow in addition to the adiabatic response, which is the same as the perturbation that would be imparted by a *massless heat sink with the negative luminosity* $-4\pi GM \chi \rho_0/\gamma$. Naturally, despite what this formulation might suggest, there is no net heat flux on to the perturber: the temperature gradient vanishes in the vicinity of the latter, and so does the heat flux.

Recently, [Eklund & Masset \(2017\)](#) have studied the evolution of the eccentricity and inclination of low-mass planets in radiative discs. They found that luminous planets expe-

⁵ A simple manner to obtain the law of ρ'_H in the immediate vicinity of the planet (i.e. at distances much shorter than λ_c) consists in solving Eq. (59) in which we neglect the left-hand side, which represents the advective term.

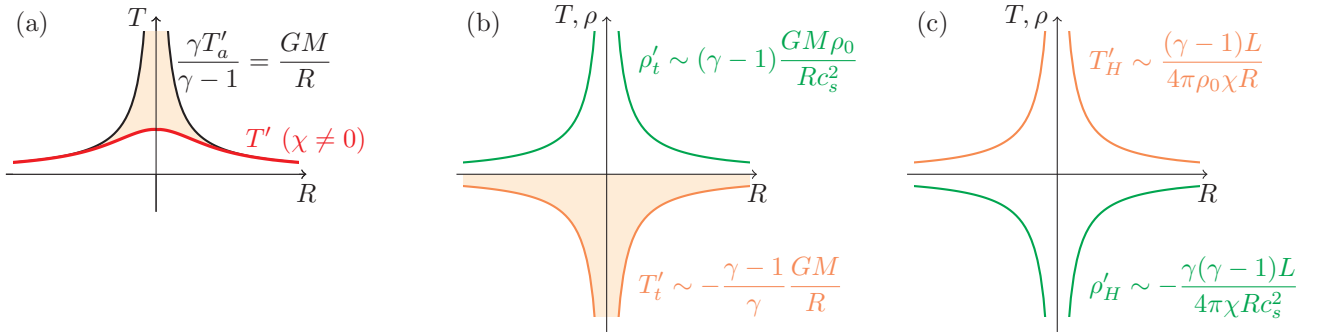


Figure 3. Schematic representation of the perturbation of temperature or density in the vicinity of the planet in various cases. The variable R denotes here the distance to the planet in an arbitrary direction. Panel (a) shows the perturbation of temperature T'_a in an adiabatic disc (black curve). The form of this perturbation comes from the fact that the perturbation of enthalpy $\gamma T'_a/(\gamma - 1)$ is nearly the opposite of the planetary potential. When thermal diffusion is introduced, the temperature profile is flattened (red curve). The new perturbation of temperature T' can then formally be written as $T'_a + T'_t$, where $T'_t < 0$ corresponds to the coloured area, and tends to the negative of T'_a when $R \rightarrow 0$. Panel (b) shows the graph of T'_t , and of the associated perturbation of density. Since the perturbation of pressure is small, we have $\rho'/\rho_0 + T'/T_0 \approx 0$, or $\rho' \approx -\gamma\rho_0 T'/c_s^2$. The shape of ρ'_t is therefore the negative of the potential, and it scales here with R^{-1} because the planetary potential does. Panel (c) shows the disturbances of density and temperature imparted by a luminous, massless perturber of luminosity L , which correspond to the heating torque. Here ρ'_H scales with R^{-1} because it obeys a diffusion equation in three dimensions around a point-like source. The comparison of the scaling of ρ'_H and ρ'_t (green curves in the electronic version) shows that the latter corresponds to the perturbation induced by a singular massless heat sink with the luminosity $-L_c$, where L_c is given by Eq. (132).

rience a growth of these orbital elements. They interpret these findings as arising from the force exerted by a hot, low-density region trailing the planet on its epicyclic or vertical motion. They also found that non-luminous planets, when embedded in radiative discs, experience a faster decay of eccentricity and inclination than in an adiabatic disc. These findings are compatible with these planets having on the contrary a cold, dense trail that contribute to damp these orbital elements, in addition to the well-known action of the coorbital Lindblad resonances (Artymowicz 1993) and coorbital vertical resonances (Artymowicz 1994), much as we would expect if the planet imparted on the flow an additional perturbation similar to that arising from a heat sink. We also note that Eklund & Masset (2017) used the same disc parameters as Benítez-Llambay et al. (2015). Their fiducial planet has therefore the same, small value of L_c (see section 5.3.2), and all the planetary luminosities that they consider exceed L_c , explaining why all their luminous planets have finite eccentricity and inclinations are larger times.

5.8 Relationship with the corotation torque

Although the perturbations of density that give rise to the thermal torques are located in the coorbital region, the thermal torques are not corotation torques. Corotation torques correspond to the exchange of angular momentum at a corotation resonance between the perturber and the disc. The equation that governs heat diffusion is parabolic, its solution is not wave-like, and a resonant behaviour is impossible.

The derivation presented here is based on a linear decomposition of the flow's perturbation, and applies in the limit of small planetary mass. Even in this limit, the flow may eventually exhibit non-linearities, with a potentially large impact on the torque: Paardekooper & Papaloizou (2009) have found that, in a disc with a sufficiently small viscosity, the corotation torque changes its value over a long

time-scale: it adopts initially, over a dynamical time-scale, the value given by linear theory, then switches to a different value, given by the (non-linear) horseshoe drag, after a time-scale which roughly corresponds to the duration of a horseshoe U-turn⁶. The smaller the planet mass, the longer it takes to perform a horseshoe U-turn and therefore to reach the non-linear regime, but this regime is eventually attained regardless of the planet mass.

Although the flow may eventually become non-linear in the coorbital region of a low-mass planet in a disc with thermal diffusion, the thermal torques should be largely insensitive to this effect, which should only affect the corotation torque. One may compare the time-scale of the U-turn (Baruteau & Masset 2008; Paardekooper & Papaloizou 2009)

$$\tau_{\text{U-turn}} \sim 10\Omega_p^{-1} \left(\frac{q}{h^3}\right)^{-1/2}, \quad (149)$$

to the response time of the thermal torques: $\tau_{\text{th}} \sim \lambda_c^2/\chi \sim \Omega_p^{-1}$. For the largely sub-thermal planets considered in this work, the last factor in Eq. (149) may be substantial, and we expect to have typically $\tau_{\text{U-turn}} \sim 10^2\Omega_p^2$, two orders of magnitude larger than the time it takes to establish the thermal torque. The horseshoe motion can thus be considered frozen over the short time-scale required for the heat released at a given instant by the planet to yield a thermal torque, which should therefore be insensitive to the horseshoe dynamics. This can also be expected on intuitive grounds: the perturbation of velocity in the coorbital region is much smaller than the unperturbed velocity, which is primarily responsi-

⁶ Over even longer time-scales, the corotation torque may exhibit an oscillatory behaviour, and it eventually converges to an asymptotic value.

ble for the distortion of the hot region that gives rise to the thermal torque.

6 CONCLUSIONS

We find that a finite thermal diffusivity changes significantly the torque experienced by a low-mass planet embedded in a gaseous protoplanetary disc. We provide an expression, Eq. (136), for the difference between the torque experienced in a disc with thermal diffusion and an adiabatic disc, when the planet does not release heat into the disc. We call this new torque component the cold thermal torque. It arises from two low-temperature, dense lobes on each side of corotation. Each one exerts on the planet a torque comparable to the so-called one-sided Lindblad torque exerted by the outer and inner legs of the pressure-supported wake. Much like this wake's torque, the outer disturbance exerts a negative torque, while the inner one exerts a positive torque. The residual torque, however, is markedly different. While the relative imbalance of the wakes' torques is of the order of the disc's aspect ratio h , the imbalance of the thermal torques is set by the ratio of the offset to corotation to the size of the lobes $\lambda_c \sim \sqrt{\chi/\Omega_p}$. This ratio is usually a quantity larger than h , which implies that the cold thermal torque is the dominant component of the torque, at least for sufficiently small planetary masses. We find, by comparing our analytic expectations to the only numerical evidence of the cold thermal torques published so far (Lega et al. 2014), that the cold thermal torque measured in the simulations has an absolute value smaller than that of the analytic estimate, even more so as the planetary mass increases. This suggests that the cold thermal torque is cut-off for planetary masses above the Earth's mass, and that full fledged thermal torques have not yet been obtained in numerical simulations.

When the planet is luminous, the heat released in the surrounding nebula obeys an equation of advection and diffusion, in which the advection stems from the Keplerian shear. The relative perturbations of density and temperature associated with the heat release have opposite values, while the pressure remains essentially unperturbed. The perturbation of density associated with the heat release, in steady state, is asymmetric when the planet is offset from corotation. We work out an expression for the net torque corresponding to this perturbation, or heating torque, given by Eq. (144). This expression is exact in the limit of an offset to corotation small compared to the size of the disturbance, and of a size of disturbance small compared to the thickness of the disc. The total torque is the given by Eq. (143). As for the cold thermal torque, the comparison of our analytic expectations to the values of the heating torque reported by Benítez-Llambay et al. (2015) suggests a cut-off above a fraction of an Earth mass.

Our analysis has assumed the planet to be on a fixed circular orbit. When the planet's luminosity is large, it can acquire a significant eccentricity, and the time averaged total torque exerted on the planet may depart significantly from the circular estimate (Eklund & Masset 2017).

The decay of the thermal torques below their analytic value for planetary masses above typically one Earth-mass is not included in the analytic formulation presented here,

based on linear perturbation theory. Studying the regime of larger planetary masses requires to deal with non-linear flows, and will likely require to be tackled through numerical simulations. This now appears as the most important step towards an integration of the thermal torques into a general torque formula.

ACKNOWLEDGEMENTS

The author acknowledges UNAM's PAPIIT grant 101616.

REFERENCES

- Alexiades V., Amiez G., Gremaud P.-A., 1996, *Communications in Numerical Methods in Engineering*, 12, 31
- Artymowicz P., 1993, *ApJ*, 419, 166
- Artymowicz P., 1994, *ApJ*, 423, 581
- Baruteau C., Masset F., 2008, *ApJ*, 672, 1054
- Benítez-Llambay P., Masset F., Koenigsberger G., Szulágyi J., 2015, *Nature*, 520, 63
- Bitsch B., Johansen A., Lambrechts M., Morbidelli A., 2015, *A&A*, 575, A28
- Cassen P., Woolum D. S., 1996, *ApJ*, 472, 789
- Eklund H., Masset F. S., 2017, *MNRAS*, 469, 206
- Fung J., Artymowicz P., Wu Y., 2015, *ApJ*, 811, 101
- Fung J., Masset F., Lega E., Velasco D., 2017, *AJ*, 153, 124
- Jiménez M. A., Masset F. S., 2017, preprint, ([arXiv:1707.08988](https://arxiv.org/abs/1707.08988))
- Lega E., Crida A., Bitsch B., Morbidelli A., 2014, *MNRAS*, 440, 683
- Lega E., Morbidelli A., Bitsch B., Crida A., Szulágyi J., 2015, *MNRAS*, 452, 1717
- Masset F. S., Casoli J., 2010, *ApJ*, 723, 1393
- Masset F. S., Velasco Romero D. A., 2017, *MNRAS*, 465, 3175
- Masset F. S., D'Angelo G., Kley W., 2006, *ApJ*, 652, 730
- Narayan R., Goldreich P., Goodman J., 1987, *MNRAS*, 228, 1
- Ormel C. W., Kuiper R., Shi J.-M., 2015a, *MNRAS*, 446, 1026
- Ormel C. W., Shi J.-M., Kuiper R., 2015b, *MNRAS*, 447, 3512
- Paardekooper S.-J., Papaloizou J. C. B., 2009, *MNRAS*, 394, 2283
- Paardekooper S., Baruteau C., Kley W., 2011, *MNRAS*, 410, 293
- Ward W. R., 1997, *Icarus*, 126, 261

APPENDIX A: SOLUTION OF THE DIFFERENTIAL SYSTEMS

We seek finite solutions of Eqs. (75)-(76) or Eqs. (94)-(95). These solutions are such that the real part has the parity of the forcing function [$\delta(X)$ in the first case, $\delta'(X)$ in the second one], whereas the opposite holds for the imaginary part. Hence, $X \mapsto R_K(X)$ and $X \mapsto i_K(X)$ are even functions of X , while $X \mapsto I_K(X)$ and $X \mapsto r_K(X)$ are odd functions of X .

Integrating Eq. (75) from $-\epsilon$ to $+\epsilon$ and taking the limit $\epsilon \rightarrow 0$, we find that

$$R'_K(0^+) - R'_K(0^-) = 2R'_K(0^+) = -1. \quad (\text{A1})$$

A similar integration of Eq. (76) yields that I'_K is continuous in 0. Since this function is even in X , this implies that $I''_K(0) = 0$ [I'_K cannot be singular in 0, as per Eq. (76)], and therefore that $I_K(0) = 0$.

Similar considerations apply to Eqs. (94) and (95). Integration of Eq. (95) with the requisite that i_K is even implies

that $i'_K(0) = 0$. Similarly, integration of Eq. (94) on a neighbourhood of 0 yields

$$r_K(\epsilon) \rightarrow \frac{\text{sgn}(\epsilon)}{2K} \quad \text{for } \epsilon \rightarrow 0 \quad (\text{A2})$$

We start our integration at a large value X_∞ of X , and integrate backwards. We consider the two initial conditions $[R_K(X_\infty), I_K(X_\infty)] = (1, \pm 1)$. We adopt for the first derivatives the approximate values

$$R'_K(X_\infty) = \sqrt{\frac{X_\infty}{2K}} [R_K(X_\infty) - I_K(X_\infty)] \quad (\text{A3})$$

$$I'_K(X_\infty) = \sqrt{\frac{X_\infty}{2K}} [R_K(X_\infty) + I_K(X_\infty)]. \quad (\text{A4})$$

We then adopt the linear combination of our two solutions that verifies $R'_K(0) = -1/(2K)$ and $I_K(0) = 0$, and we check in X_∞ that the solution is vanishingly small compared to its value at the origin. Namely we check that $|R_K(X_\infty) + iI_K(X_\infty)| < 10^{-9}|R_K(0) + iI_K(0)|$, and increase X_∞ and repeat the operation until this condition is satisfied. We have found that our solution, except in the vicinity of X_∞ where it is vanishingly small, is largely insensitive to our choice of first derivatives in X_∞ . We have found that a suitable choice for X_∞ is

$$X_\infty = 25 \quad \text{if } K > 3 \quad (\text{A5})$$

$$= 17K^{1/3} \quad \text{otherwise} \quad (\text{A6})$$

We use a similar method to solve Eqs. (94)-(95), which differ only by the forcing term in $X = 0$, except that we adopt the linear combination of our solutions that verifies $r_K(0^+) = 1/(2K)$ and $i'_K(0) = 0$.

APPENDIX B: NUMERICAL EVALUATION OF THE INTEGRALS OF F AND J

The functions $K \mapsto F(K)$ and $K \mapsto J(K)$ are defined respectively by the integrals that appear in Eqs. (81) and (99). These two functions admit simple approximations in the limit $K \rightarrow 0$ and $K \rightarrow \infty$. We therefore perform the calculation of the integrals as follows:

- We integrate over an interval $[K_{\min}, K_{\max}]$, with $K_{\min} \ll 1$ and $K_{\max} \gg 1$, where the value of I_K or i_K is obtained using the method described in Appendix A.
- We add the contribution of the intervals $[0, K_{\min}]$ and $[K_{\max}, +\infty]$ in an analytical manner, using the approximations respectively at small and large K .

In the limit $K \rightarrow \infty$, we have the approximation

$$I_K(X) \approx \frac{X + X^2}{8K^2} \exp(-X), \quad (\text{B1})$$

so that

$$F(K) \xrightarrow{K \rightarrow \infty} \frac{1}{16K^2}. \quad (\text{B2})$$

In the limit $K \rightarrow 0$, the solution $R_K(X) + iI_K(X)$ tends to the solution z_1 of the equation

$$-iXz = Kz'' + \delta(x). \quad (\text{B3})$$

The solution z_1 can itself be written in terms of the solution z_0 of the equation

$$-ixz = \frac{d^2z}{dx^2} + \delta(x), \quad (\text{B4})$$

as:

$$z_1(X) = K^{-2/3} z_0(XK^{-1/3}), \quad (\text{B5})$$

In the limit of $K \rightarrow 0$ the integral will therefore tend to

$$F(K) \xrightarrow{K \rightarrow 0} \int_{X>0} \Im[Z_K(X)] dX \quad (\text{B6})$$

$$= K^{-1/3} \int_{x>0} \Im[z_0(x)] dx \quad (\text{B7})$$

We find, using a shooting method similar to that of Appendix A:

$$\int_{x>0} \Im[z_0(x)] dx \approx 0.372 \quad (\text{B8})$$

For the evaluation of $J(K)$, we use

$$i_K(X) \xrightarrow{K \rightarrow \infty} \frac{1 + X + X^2}{8K^2} \exp(-X), \quad (\text{B9})$$

so that

$$J(K) \xrightarrow{K \rightarrow \infty} \frac{1}{8K^2} \quad (\text{B10})$$

and, for $K \ll 1$,

$$J(K) \approx \frac{0.469}{K^{2/3}}. \quad (\text{B11})$$

We obtain:

$$\int_0^\infty F(K) dK \approx 0.205 \quad (\text{B12})$$

$$\int_0^\infty F(K^{2/3}) dK \approx 0.252 \quad (\text{B13})$$

$$\int_0^\infty J(K^{2/3}) dK \approx 0.616 \quad (\text{B14})$$

APPENDIX C: ENTHALPY NEAR THE PLANET

The derivation of the cold thermal torque requires the knowledge of the enthalpy distribution in the planet's vicinity in the adiabatic case. We have made the approximation that the enthalpy is the negative of the planetary potential. We assess here the degree of accuracy of this simplifying assumption. There is an indirect albeit simple manner to evaluate the residual value of the potential plus enthalpy near the planet. The gas parcels are subjected to an effective potential that is the sum Ψ of the planetary potential and gas enthalpy. It is therefore the depth of this effective potential well that determines the width of the horseshoe region. Should the enthalpy be exactly the negative of the potential, the effective potential would vanish and the horseshoe region would not exist. On the other hand, the fact that the horseshoe region is much more narrow than what it would be if the gas parcel were subjected only to the planetary potential (in which case the horseshoe region would have the same width as in the restricted three-body problem) indicates that the effective potential well is much more shallow than the gravitational potential well; that is, the enthalpy

is approximately the opposite of the potential. The width of the horseshoe region in an adiabatic situation gives us an idea of the residual value of the effective potential. The Bernoulli constant on the separatrix of the horseshoe region is $(3/8)\Omega_p^2 x_s^2$, where x_s is the half-width of the horseshoe region, and it is also the value of the effective potential at the stagnation point, in the vicinity of the planet (Masset et al. 2006). The effective potential well does not diverge in the vicinity of the planet and is nearly constant over the innermost pressure length-scale. We compare it to the planetary potential at the Bondi radius (which is c_s^2 , by definition). We have

$$\frac{\Psi}{c_s^2} = \frac{3}{8} \frac{\Omega_p^2 x_s^2}{c_s^2} = O(\mu/h^3), \quad (\text{C1})$$

where we have used $x_s \sim r_p(q/h)^{1/2}$. This shows that for largely sub-thermal planets, our approximation is reasonably accurate. For an Earth-mass planet in a disc with $h = 0.05$, the assumption that the enthalpy is the negative of the potential well is accurate to within $\sim 1\%$ at the Bondi radius.

APPENDIX D: ON THE HEAT SOURCE OF THE NON-LUMINOUS CASE

The Laplacian of the field p'_a is, using Eq. (130)

$$\Delta p'_a = -2\nabla\rho_o \cdot \nabla\Phi_p - \rho_o\Delta\Phi_p, \quad (\text{D1})$$

where we neglect the second-order derivative of ρ_o . We justify here why we can neglect the first term of the right-hand side of Eq. (D1). The field $\nabla\rho_o$ is uniform on the neighbourhood of the planet, while the field $\nabla\Phi_p$ is directed towards the planet. Their dot product is a non-singular field that changes sign across the planet's orbit. We can estimate the integrated heat source term L_+ of the outer part ($x > x_p$) over a volume λ_c^3 as

$$|L_+| \sim \frac{\lambda|\xi|}{\gamma} \cdot \frac{\rho_o}{r_p} \cdot \frac{GM}{\lambda_c^2} \cdot \lambda_c^3, \quad (\text{D2})$$

where $\xi = -d \log \rho_o / d \log r$, while the inner part ($x < x_p$) has a luminosity L_- similar in absolute value, and of opposite sign, to L_+ . The one-sided torques excited in the outer disc by L_+ and in the inner disc by L_- have same sign, so the net torque Γ_{\pm} arising from the term of interest is approximately twice the one-sided torque due to L_+ , which gives

$$\Gamma_{\pm} \sim 0.13(\gamma - 1) \frac{G^2 M^2 \xi \rho_o}{c_s^2} \cdot \frac{\lambda_c}{r_p}. \quad (\text{D3})$$

This is approximately $\lambda_c^2/(x_p r_p)$ times the net, cold thermal torque found in section 4. This ratio is also $\sim (\lambda_c/H)^2 \ll 1$, so the torque arising from the term under consideration is negligible, which justifies our approximation.

This paper has been typeset from a $\text{\TeX}/\text{\LaTeX}$ file prepared by the author.